Inactivation of AMPK alpha 1 Induces Asthenozoospermia and Alters Spermatozoa Morphology

Pauline Tartarin, Edith Guibert, Aminata Toure, Claire Ouiste, Jocelyne Leclerc, Nieves Sanz, Sylvain Brière, Jean-Louis Dacheux, Bernadette Delaleu, Judith R. Mcneilly, et al.

Inactivation of AMPKα1 Induces Asthenozoospermia and Alters Spermatozoa Morphology

Pauline Tartarin, Edith Guibert, Aminata Touré, Claire Ouiste, Jocelyne Leclerc, Nieves Sanz, Sylvain Brière, Jean-Louis Dacheux, Bernadette Delaleu, Judith R. McNeilly, Alan S. McNeilly, Jean-Pierre Brillard, Joëlle Dupont, Marc Foretz, Benoit Viollet, and Pascal Froment

Unité Mixte de Recherche (UMR) 6175 (P.T., E.G., C.O., S.B., J.-L.D., B.D., J.P.B., J.D., P.F.), Physiologie de la Reproduction et des Comportements (Institut National dela Recherche Agronomique/Centre National dela Recherche Scientifique/Université Tours/Haras Nationaux), 37380 Nouzilly, France; Institut National de la Santé et de la Recherche Médicale Unité 1016, Institut Cochin (A.T., J.L., N.S., M.F., B.V.); and CNRS, UMR 8104 (A.T., J.L., N.S., M.F., B.V.); and Université Paris Descartes (A.T., J.L., N.S., M.F., B.V.), Sorbonne Paris Cité, 75014 Paris, France; and Medical Research Council Human Reproductive Sciences Unit (J.R.M., A.S.M.), University of Edinburgh, Queen's Medical Research Institute, Edinburgh EH16 4TJ, Scotland, United Kingdom

AMP-activated protein kinase (AMPK), a key regulator of cellular energy homeostasis, is present in metabolic tissues (muscle and liver) and has been identified as a modulator of the female reproductive functions. However, its function in the testis has not yet been clearly defined. We have investigated the potential role of AMPK in male reproduction by using transgenic mice lacking the activity of AMPK catalytic subunit α1 gene [α1AMPK knockout (KO)]. In the testis, the α1AMPK subunit is expressed in germ cells and also in somatic cells (Sertoli and Leydig cells). α1AMPK KO male mice show a decrease in fertility, despite no clear alteration in the testis morphology or sperm production. However, in α1AMPK$^{-/-}$ mice, we demonstrate that spermatozoa have structural abnormalities and are less motile than in control mice. These spermatozoa alterations are associated with a 50% decrease in mitochondrial activity, a 60% decrease in basal oxygen consumption, and morphological defects. The α1AMPK KO male mice had high androgen levels associated with a 5- and 3-fold increase in intratesticular cholesterol and testosterone concentrations, respectively. High concentrations of proteins involved in steroid production (3β-hydroxysteroid dehydrogenase, cytochrome steroid 17 alpha-hydroxylase/17,20 lysate, and steroidogenic acute regulatory protein) were also detected in α1AMPK$^{-/-}$ testes. In the pituitary, the LH and FSH concentrations tended to be lower in α1AMPK$^{-/-}$ male mice, probably due to the negative feedback of the high testosterone levels. These results suggest that total α1AMPK deficiency in male mice affects androgen production and quality of spermatozoa, leading to a decrease in fertility. **(*Endocrinology* 153: 3468–3481, 2012)**

Interaction between energy balance and reproductive status has been investigated for several decades. In humans, anorexia and obesity can harm ovarian function and spermatogenesis (for review see Refs. 1 and 2). A modification in quantity and/or quality of nutrition in female mammals could influence ovarian cycles and the weaning-estrus interval (for review, see Ref. 3).

During the last 15 yr, several messengers of the fuel gauge have been identified to regulate fertility. Mice, deficient or overexpressing hormones produced by adipose

ISSN Print 0013-7227 ISSN Online 1945-7170
Printed in U.S.A.

doi: 10.1210/en.2011-1911 Received October 25, 2011. Accepted April 13, 2012.
First Published Online May 11, 2012

Abbreviations: ACC, Acetyl coenzyme A carboxylase; AMPK, AMP-activated protein kinase; CREB, cAMP response element-binding protein; GATA4, transcription factor GATA-4; 3βHSD, 3β-hydroxysteroid dehydrogenase; $\dot{V}O_2$, oxygen consumption; KO, knockout; LKB1, liver kinase B1; LXR, liver X receptor; MARK, microtubule affinity-regulating kinase; P450c17, cytochrome P450c17, 17 alpha-hydroxylase/17,20 lysate; PCNA, proliferation cell nuclear antigen; PGC-1α, peroxisome-proliferator-activated receptor γ coactivator 1α; RXR, retinoid X receptor; SER, smooth endoplasmic reticulum; SNRK, sucrose nonfermenting related kinase; TSSK, testis specific serine kinase; TUNEL, terminal deoxynucleotidyl transferase-mediated deoxy-UTP nick end labeling; VASA, mouse homolog Drosophila Vasa; X-gal, 5-bromo-4-chloro-3-indoyl-β-D-galactopyranoside.

tissue such as leptin, adiponectin (4, 5), or insulin signaling molecules (6, 7) show a decrease in fertility. At the cellular level, several proteins have been described as key factors involved in the relations between the energy homeostasis and reproductive functions. These proteins are nuclear receptors, kinases sensitive to the ATP to ADP ratio, or transcription factors. They are involved in the control of lipid and glucose metabolism. Several knockout (KO) mice models have shown a relationship between lipid/cholesterol metabolism and male fertility. For example, the nuclear oxysterol receptor [liver X receptor (LXR)] forms a heterodimer with the retinoid X receptor (RXR) and activates gene transcription involved in cholesterol transport such as the ATP-binding cassette transporters (8). The double knockout of α-LXR /β-LXR subunits in mice leads to a disrupted spermatogenesis and a vacuolization of seminiferous tubules growing with age. Spermatozoa present structure disturbance such as hairpin flagella and testes with high levels of intratesticular cholesterol associated with low testosterone levels (9–11). RXRβ is a nuclear receptor that interacts as a heterodimer with different nuclear receptors such as retinoic acid receptor, LXR, peroxisome proliferator-activated receptor, and modulate cholesterol transport (12). KO mice lacking RXRβ have a progressive testicular degeneration, an accumulation of lipid droplets in Sertoli cells, and altered spermatozoa due to malformations of acrosome and mitochondrial sheaths (13). Similarly, the hormone-sensitive lipase disruption, a cholesterol esterase (14), results in a marked reduction in spermatid number and severe acrosome disturbances leading to sterility (15). Thus, control of the lipid metabolism is closely connected to male gametogenesis. A key regulator of cellular energy and cholesterol homeostasis, the 5′-AMP-activated protein kinase (AMPK), has also been detected in reproductive tissue (16). AMPK plays an important role in the fatty acid and cholesterol homeostasis (17–19). Indeed, activation of AMPK inhibits expression of acetyl-coenzyme A carboxylase (ACC), fatty acid synthase (FAS), and 3-hydroxy-3-methylglutaryl (HMG)-coenzyme A reductase (HMGR), which are rate-limiting enzymes for cholesterol and fatty acid biosynthesis. AMPK also activates glucose transporter 4 (GLUT4) translocation, leading to an increase in glucose intake (for review, see Ref. 20).

This serine threonine kinase, also named protein kinase AMP-activated (PRKA) or sucrose nonfermenting 1 (SNF1), is ubiquitous, being present in plants (21), yeast (22), and the animal kingdom [fish (23), birds (24), and mammals (25)]. AMPK is a heterotrimeric complex composed of a catalytic subunit α and two regulatory subunits β and γ. The α-subunit is present in two isoforms, α1 and α2, and two and three isoforms for β- and γ-subunits, respectively. AMPK is sensitive to the AMP to ATP ratio, and its activation allows turning off of ATP-consuming processes and stimulation of catabolic pathways. Activation of AMPK requires the phosphorylation of α-subunit in threonine 172. The binding of AMP in regulatory subunits could activate AMPK directly by allosteric activation (16, 26). Upstream kinases such as liver kinase B1 (LKB1) and Ca^{2+} calmodulin-dependent protein kinase kinase 1 or 2 (CaMKK1 or CaMKK2) are clearly identified to phosphorylate AMPK (27, 28), but other upstream kinases like TGF-β-activated kinase (TAK1) (29) or kinase suppressor of Ras (KSR2) (30) could up-regulate AMPK activity. Furthermore, AMPK is activated by metabolic hormones leptin (31) and adiponectin (32), two adipokines involved in energy homeostasis and whose receptors are also expressed in the ovary and testis.

By homology analysis of the catalytic domain of the AMPK sequence, Manning *et al.* (33) identified 12 AMPK-related kinases [brain-specific kinase 1, brain-specific kinase 2, nuclear AMPK-related kinase 1, nuclear AMPK-related kinase 2, Qin-induced kinase, salt inducible kinase, QSK (also named salt-inducible kinase 3, salt-inducible kinase, microtubule affinity-regulating kinase (MARK)1, MARK2, MARK3, MARK4, and maternal embryonic leucine zipper kinase] and eight other kinases less related to AMPK [noninducible immunity 1, sucrose nonfermenting related kinase (SNRK), testis specific serine kinase (TSSK)1, TSSK2, TSSK3, TSSK4, small serine/threonine kinase, and hormonally upregulated neu-tumor associated kinase]. Most of them are activated by LKB1 (33–35) and four of these AMPK-related-kinases are found in the testis (MARK2, NIM1, SNRK, and TSSK1) (35) (36). However, the role of these AMPK-related kinases has not been clearly defined (37).

Activation of AMPK, by two synthetic drugs, 5-aminoimidazole-4-carboxamide-1-β-d-ribofuranoside (AICA riboside) or metformin (an insulin sensitizer drug), decreases steroid production in ovarian granulosa cells (38). In human granulosa cells, stimulation of adiponectin receptors (39–42) increases the IGF-I-induced steroid production (43, 44). In mouse oocytes, phosphorylation of AMPK provides a meiotic maturation signal that improves meiotic resumption (45). Overall, these studies suggest that AMPK is closely linked to female fertility.

AMPK may have a role in the control of male fertility. Indeed, all AMPK subunits are found in the rat testis; however, the α1AMPK complexes account for most (about 75%) of the total AMPK activity in the testis (16). In addition, *in vitro* incubation of Sertoli cells (the nurse cells of male germ cell lineage) with synthetic AMPK activators leads to an increase in the production of lactate, the energy substrate for germ cells (46). Moreover, in mice, the loss of activity of AMPK kinase LKB1 (47) or the AMPK-re-

lated kinase MARK2 (36) induces alteration of sperm production and morphology leading to a reduction in fertility or even sterility, suggesting possible involvement of AMPK activity in male fertility.

To test this hypothesis, we studied a transgenic mouse model inactivated for the α1AMPK subunit gene and analyzed sperm parameters and Sertoli and Leydig cell functions.

Materials and Methods

Animals

The generation and characterization of the transgenic mice have been previously described by Jørgensen *et al.* (48). Briefly, an IRES-βgeo cassette (internal ribosomal entry site-β-galactosidase and neomycin phosphotransferase fusion gene) was inserted to delete a part of the catalytic domain of α1AMPK subunit from amino acids 97–157. The genotype of the offspring was first determined by PCR as described previously (48). Mice were maintained under standard conditions of light (12 h light, 12 h darkness) and temperature with *ad libitum* access to food and water. Animal studies described herein were reviewed and approved (agreement no. 75-886) by the Directeur Départemental des Services Vétérinaires of the Préfecture de Police de Paris. The fertility assessment was estimated by counting the number of pups per litter of the following breeding: male α1AMPK$^{+/-}$ mated with female α1AMPK$^{+/-}$, male α1AMPK$^{-/-}$ mated with female α1AMPK$^{+/-}$, and male α1AMPK$^{-/-}$ mated with female α1AMPK$^{-/-}$.

Blood collection and tissue removal

Blood samples were recovered by intraorbital puncture in EDTA, centrifuged for 15 min at 3000 $\times$ *g*, and plasma was stored at −20 C. For both genotypes, animals were killed by cervical dislocation, and liver, pituitary, epididymis, testes, and spermatozoa were immediately recovered and fixed in Bouin solution for histological studies or stored at −80 C. Total body weight was averaged before killing, and testes were weighed immediately after recovery.

Morphometry of testis

The testis volume was obtained using the formula: 0.71 $\times$ length $\times$ width^2 (49). Testes, once fixed, were processed in paraffin and serially sectioned at 7 μm slice thickness. Round transverse sections of seminiferous tubules diameters (n = 20 measurements per animal, with five α1AMPK$^{+/+}$ and six α1AMPK$^{-/-}$ mice) were measured for each testis using an ocular measuring device (50).

Leydig cell morphometry

The percent volume occupied by the Leydig cell nuclei was counted in 25 randomly selected areas per animal, using a 441-point square lattice at ×400 magnification. Because the Leydig cell nucleus is spherical, the volume of the nucleus of a single Leydig cell was estimated from the equation for the volume of a sphere ($4/3 \times \pi \times r^3$, where r is the radius of the nucleus of the cell). The total number of Leydig cells per testis was determined from the volume occupied by all Leydig cell nuclei in the testis volume and divided by the mean Leydig cell nucleus volume. Individual Leydig cell volume was obtained from the nucleus volume and the nucleus to cytoplasm ratio. For each animal, 45–85 Leydig cells per testis section were measured. The mean volume of the Leydig cells was calculated as described previously (51).

Isolation of testicular cells

The preparation of spermatogonia, spermatocytes, spermatids, and peritubular and Leydig cells used in Fig. 1 was described by Toure *et al.* (52), and Sertoli cells were prepared from 20-d-old mice as described previously by Froment *et al.* (53). Mouse Sertoli cells were cultured at 2×10^5 cells per well in six-well dishes in HEPES-buffered F12/DMEM (Sigma Chemical Co., St. Louis, MO) added to 1% fetal calf serum (PAA Laboratories GmbH, Pasching, Austria) at 33 C in a humidified atmosphere of 5% CO2 in air. The medium was changed every 48 h. Cells were stimulated for 15 min with 100 ng/ml ovine FSH (Sigma) or for 48 h with 5 mM metformin (Sigma).

Histochemical staining for β-galactosidase activity

Testes were fixed in 4% paraformaldehyde in PBS for 1 h and then embedded in Tissue-Tek O.C.T., frozen at −80 C, and cut into 10-μm sections with a cryostat. The sections were washed with PBS, incubated in PBS containing 2 mM $MgCl_2$, 5 mM $K_3Fe(CN)_6$, 5 mM $K_4Fe(CN)_6$, and 1 mg/ml 5-bromo-4-chloro-3-indoyl-β-D-galactopyranoside (X-gal) at 30 C for 24 h. The procedure for X-gal staining has been previously described by Papaioannou and Johnson (54). Negative controls took the form of α1AMPK$^{+/+}$ mice.

Immunohistochemistry

Testes embedded in paraffin were serially sectioned at 7 μm slice thickness. Deparaffinized sections were hydrated, microwaved for 5 min in an antigen unmasking solution (Vector Laboratories, Inc., AbCys, Paris, France), and left to cool to room temperature. The sections were then washed in a PBS bath for 5 min, and to quench endogenous peroxidase activity, they were immersed in peroxidase blocking reagent for 10 min at room temperature (Dako Cytomation, Dako, Ely, UK). After two PBS baths for 5 min, nonspecific background was prevented by incubation in 5% lamb serum/PBS for 30 min. Finally, sections were incubated overnight at 4 C with PBS containing primary antibody against phospho-ACC (Ser79) (1:200; Upstate Biotechnology Inc., Lake, Placid, NY), mouse homolog Drosophila Vasa (VASA) (1:200; AbCam, Cambridge, MA), transcription factor GATA-4 (GATA4) (1:200; Santa Cruz Biotechnology, Santa Cruz, CA), proliferation cell nuclear antigen (PCNA) (1:500; Santa Cruz), and phospho-cAMP response element-binding protein (CREB) (Ser 133) (1:100; Cell Signaling Technologies, Beverly, MA). The next day, after two PBS baths for 5 min, sections were incubated with a ready-to-use labeled polymer-horseradish peroxidase antirabbit or antimouse for 30 min at room temperature (Dako Cytomation Envision Plus HRP system; Dako, Ely, UK). Finally, after two baths in PBS, staining was revealed by incubation with 3,3′-diaminobenzidine at room temperature (Sigma Fast diaminobenzidine tablet dissolved in deionized water; Sigma). Negative controls were incubated with rabbit or mouse IgG (data not shown).

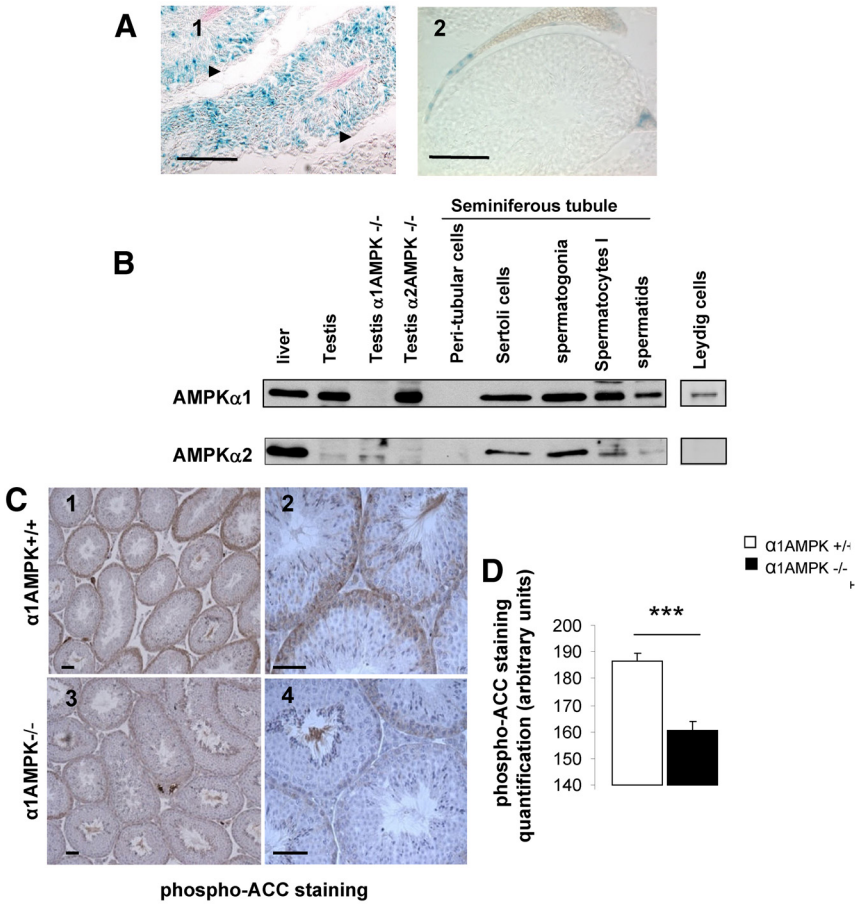

FIG. 1. Expression of α1AMPK in testis. A1 and A2, Analysis of the β-galactosidase activity and expression in the testis (gene reporter inserted in α1AMPK gene) (48) (*black arrowheads* localized peritubular cells); A2, negative controls were analyzed in α1AMPK wild-type mice (absence of the gene reporter). *Scale bar*, 20 μm. B, Western blot analysis of α1AMPK and α2AMPK subunits in the whole testis and different testicular cells in wild-type mice or α1AMPK$^{-/-}$, α2AMPK$^{-/-}$ mice (testis α1AMPK$^{-/-}$, testis α2AMPK$^{-/-}$), respectively. Liver was used as positive control (lane 1). C, Immunohistochemical staining of phospho-ACC in α1AMPK wild-type testis section (1 and 2) and in α1AMPK KO testis section (3 and 4). *Scale bar*, =20 μm. D, Quantification of the phospho-ACC staining intensity. Data are represented as means ± SEM (n = 3). ***, $P < 0.001$.

The intensity of phospho-ACC and phospho-CREB staining was estimated by using the software Scion Image version 4.02 (Scion Corp., Frederick, MD). At least 50 measurements of a 25-μm^2 area from different sections per animal (three animals per genotype) were made, and the mean result is expressed in arbitrary units.

Detection of apoptosis

Deparaffinized sections were hydrated, permeabilized with proteinase K, and the *in situ* end labeling of nuclear DNA fragmentation was performed as described in the instruction manual (FragEL kit; Calbiochem, VWR, West Chester PA). Negative controls were terminal deoxynucleotidyl transferase free.

Sperm head counts

Testes and epididymis were thawed and cut into 2-mm pieces. To isolate spermatozoa and elongated spermatid heads from the other cells, samples were then suspended in 1 ml 0.15 M NaCl, 0.05% Triton X-100 buffer. Samples were homogenized and sonicated for 30 sec. Sperm heads were counted with a hemocytometer, and after correction for sample volume and tissue weight, the concentration was determined as previously described by Jégou *et al.* (55).

Sperm morphology and motility analysis

The cauda epididymis was cut into small pieces in M2 medium (Sigma) supplemented with 1% BSA; the sperm released into the medium were incubated 10–15 min at 37 C in 5% CO_2 to allow sperm diffusion. At least 120 spermatozoa per animal were analyzed and classified as normal or atypical (microcephalic, curved spermatozoa, irregular head, or thinned head). The sperm suspension was also diluted for quantitative assessment of motility using a Hamilton-Thorne motility analyzer (Hamilton-Thorne Biosciences, Beverly, MA). For each sample, sperm curvilinear velocity and sperm straight-line velocity parameters were measured as indicators of sperm movement. For each mouse (n = 6), 1000 spermatozoa were analyzed at 37 C in 100-μm standard counting chambers (Leja, IMV Technologies, Aigle, France).

Mitochondrial activity

Mitochondrial activity was determined by JC-1 staining (Invitrogen, Cergy-Pontoise, France). Fresh epididymal semen was incubated with 2 μM JC-1-M2 medium for 15 min at 37 C, and then spermatozoa were washed and examined using standard immunofluorescence microscopy (at least 150 spermatozoa per animal were analyzed). A green fluorescence emission was detected in the presence of low mitochondrial membrane potential, and an orange/red fluorescence was emitted in mitochondria with high membrane potential.

Determination of sperm mitochondrial oxygen consumption (JO_2)

Spermatozoa were collected in M2 medium supplemented with 5 mM sodium pyruvate according to the method previously described by Mukai and Okuno (56) and were resuspended at a density of 2×10^6 spermatozoa/ml. The JO_2 (picomoles O_2 per second per 10^6 cells) of the cell suspension was recorded at 37 C with an Oroboros Oxygraph-2k (Oroboros, Innsbruck, Austria), and data were acquired with DatLab4 software. Basal cell respiration was determined, and then oligomycin (0.5 μg/ml) and increasing concentrations of carbonyl cyanide *m*-chlorophenylhydrazone (1–2 μM) were subsequently added to determine the oligomycin-sensitive JO_2 (basal JO_2 minus oligomycin-insensitive JO_2), which represents the cellular oxygen consumption related to ATP synthesis and the maximal (uncoupled) respiratory rate, respectively.

Transmission electron microscopy

Testes (n = 4 mice in each genotype) and spermatozoa (n = 6 mice in each genotype) were fixed in 4% glutaraldehyde, 0.1 M sodium cacodylate buffer (Sigma) (pH 7.4) for 24 h at 4 C, postfixed in 1% osmium tetroxide, and embedded in Eponaraldite resin. For ultrastructure analysis, samples were serially sectioned at 70 nm slice thickness, placed on 200-mesh copper grids, and stained with uranyl acetate followed by lead citrate. Finally, sections were examined on a CM10 electron microscope (CM 10; Philips, Eindhoven, The Netherlands). Analysis software was used for image acquisition (Soft Imaging System, Olympus, Münster, Germany), and 40 and 80 spermatozoa in α1AMPK$^{+/+}$ and α1AMPK$^{-/-}$ mice, respectively, and more than 2000 mitochondria per genotype were analyzed and classified as normal or exhibiting partial/total cristolysis.

Oxidative stress

The total antioxidant capacity of testicular cell lysates was evaluated by using the Cayman's antioxidant assay kit according to the instruction manual (Cayman, Interchim, Montluçon, France). This assay is based on the ability of antioxidants (vitamins, proteins, lipids, glutathione, uric acid, *etc.*) to inhibit the oxidation of 2,2′-azino-bis(3-ethylbenzthiazoline-6-sulfonic acid. Total antioxidant capacity was expressed as Trolox equivalent antioxidant capacity per milligram of testis.

Western immunoblotting

Lysates of liver, testis, epididymis, or isolated testicular cells (described above), and the protein analysis by immunoblot assay were described previously (50). Protein concentration was measured by a colorimetric assay (DC assay kit; Uptima Interchim, Montluçon, France).

Primary antibodies against α1AMPK and α2AMPK were a kind gift from G. Hardie (University of Dundee, Dundee, UK), 3β-hydroxysteroid dehydrogenase (3βHSD) and cytochrome P450c17 (P450c17, 17 alpha-hydroxylase/17,20 lysate) were purchased from Santa Cruz Biotechnology, phospho-CREB (Ser 133) from Cell Signaling Technologies, and tubulin and vinculin from Sigma. The anti-steroidogenic acute regulatory protein (StAR) and anti-p450scc (cholesterol side-chain cleavage enzyme) antibodies were generously provided by Dr. Dale Buchanan Hales (Department of Physiology and Biophysics, University of Illinois at Chicago, Chicago, IL). All antibodies were used at 1/1000 dilution in Western blotting, except 3βHSD and phospho-CREB antibodies diluted at 1:500. The signal was detected with horseradish peroxidase conjugated with specific secondary antibody followed by an enhanced chemiluminescence reaction.

The band densities were estimated by using the software Scion Image version 4.0.2. The results are expressed as the signal intensity in arbitrary units and correspond to the average of three cell lysate signals per genotype after normalization by an internal standard (tubulin or vinculin).

Hormone assay

Testosterone and cortisol concentrations were assessed by RIA in duplicate as previously described (57, 58). For testosterone assay, a sensitivity test was 15 pg/tube and intraassay coefficients of variation of 5.3%. The sensitivity of the cortisol assay was 0.25 ng/ml, and the intraassay of variation was 6.6% at 4 ng/ml. Concentrations of LH and FSH in plasma and pituitary extracts were determined by RIA using reagents supplied by the National Institute of Diabetes and Digestive and Kidney Diseases (Bethesda, MD) (rLH: rLH-RP-3; rFSH: rFSH-RP-2) as described by McNeilly and colleagues (59, 60). The sensitivity was 0.1 ng/ml (LH) and 1 ng/ml (FSH), and the intraassay coefficients of variation were less than 5%.

Lactate, cholesterol, and cAMP assay

Lactate and cholesterol concentrations were determined according to commercial spectrophotometric assays (Sigma Diagnostics procedure no. SELACT02 from Sigma, l'Isle d'Abeau Chesnes, France; cholesterol RTU, TG PAP 150 from BioMerieux, Marcy l'Etoile, France). cAMP concentration was measured by cAMP-Glo Assay (Promega, Madison, WI). Each standard and sample was assessed in duplicate.

Statistical analysis

All data are presented as the mean ± SEM. Student's *t* test was used to compare means between α1AMPK KO samples and their corresponding control. In the case of multiple comparisons of means, statistical analysis was performed by ANOVA followed by the Newman-Keuls test. Probability values ≤ 0.05 were considered significant.

Results

Alteration of fertility in male α1AMPK$^{-/-}$ mice

Adult males lacking the activity of α1AMPK have shown a significant decrease in fertility, as attested by the number of pups per litter when α1AMPK KO males were crossed with α1AMPK$^{+/-}$ females in comparison with α1AMPK$^{+/-}$ males (5.1 ± 0.5 *vs.* 6.7 ± 0.5 pups per litter, respectively, Table 1). α1AMPK$^{-/-}$ males crossed with

TABLE 1. α1AMPK$^{-/-}$ male mice present a reduced fertility

Genotype	Males (n)	Females (n)	Litter	Pups	Pups per litter
Male α1AMPK$^{+/-}$ × female α1AMPK$^{+/-}$	10	19	36	240	6.7 ± 0.5
Male α1AMPK$^{-/-}$ × female α1AMPK$^{+/-}$	14	28	21	107	5.1 ± 0.5[a]
Male α1AMPK$^{-/-}$ × female α1AMPK$^{-/-}$	21	22	29	133	4.6 ± 0.4[b]

Results are means of pups per litter of the following breeding: male α1AMPK$^{+/-}$ mated with female α1AMPK$^{+/-}$ (line 1), male α1AMPK$^{-/-}$ mated with female α1AMPK$^{+/-}$ (line 2), and male α1AMPK$^{-/-}$ mated with female α1AMPK$^{-/-}$ (line 3). Data are represented as mean ± SEM.

[a] $P < 0.05$ for line 1 *vs.* line 2.

[b] $P < 0.001$ for line 1 *vs.* line 3.

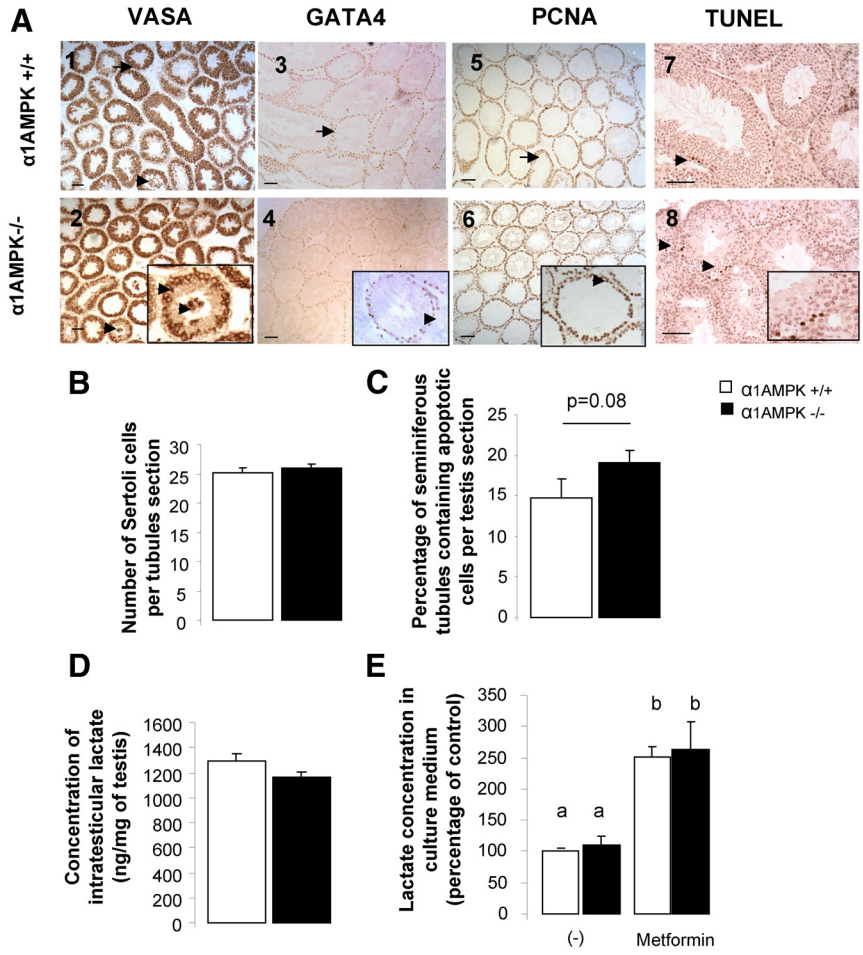

FIG. 2. Histological analysis of α1AMPK$^{-/-}$ testis. A, Testicular sections immunostained against VASA (1 and 2), GATA4 (3 and 4), PCNA (5 and 6), and apoptotic DNA fragmentation (7 and 8) from α1AMPK$^{+/+}$ mice (1, 3, 5, and 7) and α1AMPK$^{-/-}$ mice (2, 4, 6, and 8). *Scale bar*, 50 μm. All stages of spermatogenesis were visible, and no clear alteration was observed. Few germ cells sloughing were observed in both genotypes (*arrows* in A1 and A2). B, Quantification of GATA4-immunoreactive cells in seminiferous tubule (20 tubules per animal, n = 4 mice). C, Percentage of seminiferous tubules with at least one TUNEL-positive nuclei (n = 4 mice). D, Lactate concentration, an energy substrate for spermatozoa, in α1AMPK$^{+/+}$ and α1AMPK$^{-/-}$ testis (n = 5). E, Lactate secretion measured in culture medium conditioned by α1AMPK$^{+/+}$ and α1AMPK$^{-/-}$ Sertoli cells for 48 h in the presence or absence of 5 mM metformin (percentage of control normalized per 200,000 cells/wells). Data are represented as means ± SEM (n = 3 in triplicate). a and b, Significant differences.

α1AMPK$^{-/-}$ females presented a stronger decrease in fertility (4.6 ± 0.4 pups per litter). The α1AMPK gene in transgenic mice (48) was disrupted by insertion of the reporter gene β-galactosidase, allowing us to localize the expression of α1AMPK in the testis by X-gal staining (Fig. 1A). α1AMPK is expressed in Leydig cells, Sertoli cells, and in germ cells (Fig. 1). α1AMPK was also detected in epithelium of the epididymal ducts (Supplemental Fig. 1, published on The Endocrine Society's Journals Online web site at http://endo.endojournals.org). Absence of α1AMPK expression in the testis of α1AMPK$^{-/-}$ mice was confirmed by Western blot using α1 antibody (Fig. 1B); consistent with this, we observed a reduction of the phospho-ACC-immunoreactive cells in seminiferous tubules, one of the major downstream targets of AMPK ($P < 0.001$) (Fig. 1, C and D). α2AMPK is present in the testis at a lower level (Fig. 1B).

As previously reported, the average body and testis weight in α1AMPK KO mice is similar to those of wild mice (61) (Supplemental Table 1). Morphological analysis of testis and epididymis (Fig. 2A and Supplemental Fig. 1) has not shown clear alteration of structure and polarity between the two genotypes.

Alteration of spermatozoa in male α1AMPK$^{-/-}$ mice

To identify the cause of reduced fertility, an analysis of the testis cell composition by using a specific cell marker of germ cells (VASA-immunoreactive cells) and their nurse cells, the Sertoli cells (GATA4-immunoreactive cells), was performed and did not show alteration in α1AMPK KO mice (Fig. 2, A1–A4 and B). Evaluation of cell proliferation and apoptosis was assayed by immunostaining of the PCNA, and of terminal deoxynucleotidyl transferase-mediated deoxyUTP nick end labeling (TUNEL). No clear difference in proliferation (including mono- and multilayer of PCNA-positive cells in seminiferous tubules), and apoptosis was noticed (Fig. 2, A5–A8 and C). The lactate concentration produced by the Sertoli cells representing the main energetic substrate for spermatozoa was also measured. No difference was observed in testicular extract between each genotype (Fig. 2D) in 48 h culture medium conditioned by α1AMPK$^{+/+}$ and α1AMPK$^{-/-}$ Sertoli cells, even after metformin stimulation (Fig. 2E).

Our finding of α1AMPK expression in spermatozoa (Fig. 3A) led us to investigate the production and quality of α1AMPK$^{-/-}$ sperm. The numbers of spermatids and spermatozoa heads in testes and in cauda epididymis of wild-type and mutant mice were compared and did not show alteration (Fig. 3, B and C). However, α1AMPK KO spermatozoa had twice as many head abnormalities as α1AMPK wild-type counterparts (α1AMPK$^{-/-}$ mice, 48% of abnormal sperm heads; α1AMPK$^{+/+}$ mice, 26%; $P < 0.01$; Fig. 3D), but flagellum length was not altered (data not shown). Only ab-

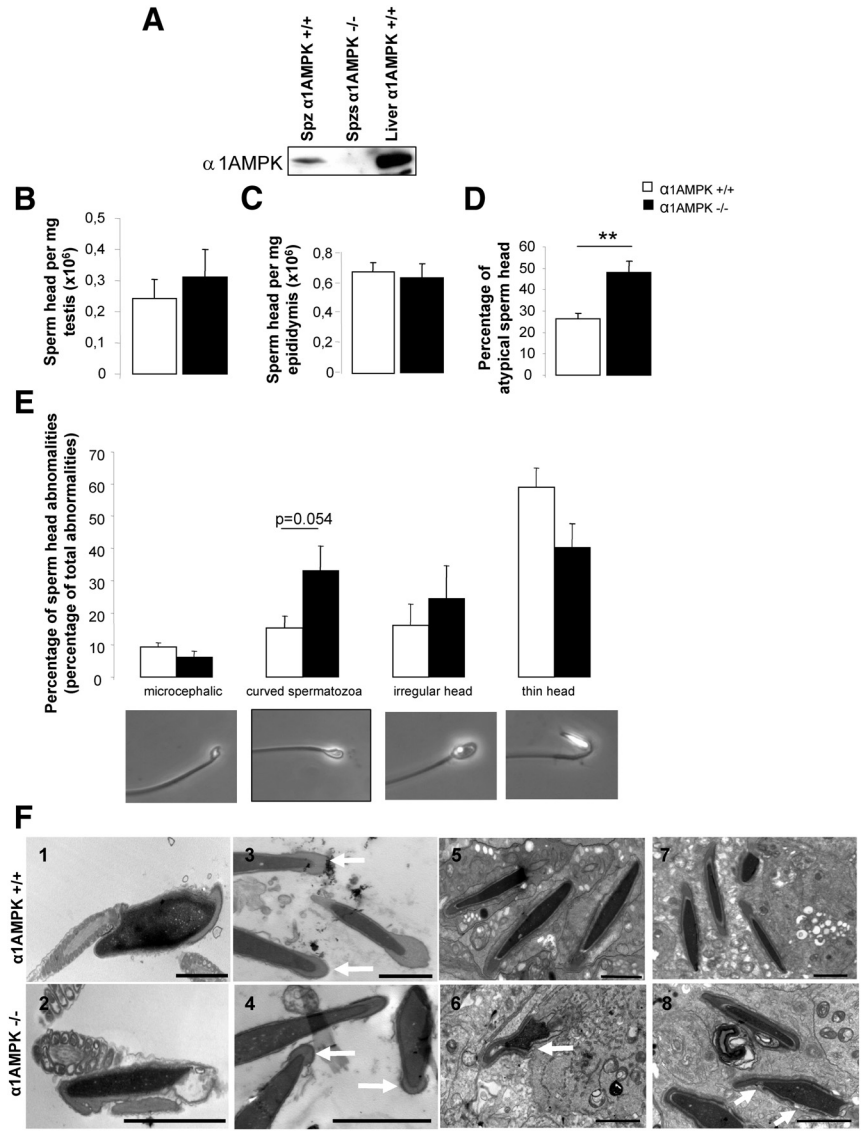

FIG. 3. Alteration of spermatozoa morphology in male α1AMPK$^{-/-}$ mice. A, Expression of α1AMPK subunits protein in spermatozoa extract purified from α1AMPK$^{+/+}$ and α1AMPK$^{-/-}$ epididymis. Liver was used as positive control. B and C, Number of sperm head per milligram of testis (B) and per milligram of cauda epididymis (C) from α1AMPK$^{+/+}$ mice (n = 4) and α1AMPK$^{-/-}$ mice (n = 4). D, Percentage of atypical sperm head in both genotypes. **, $P < 0.01$. E, Classification of sperm head abnormalities in α1AMPK$^{+/+}$ mice (n = 5) and α1AMPK$^{-/-}$ mice (n = 5) in microcephalic, curved spermatozoa, irregular head, and thin head. Representative micrographs are presented under the bar graph. Data are represented as mean or percentage ± SEM. F, Transmission electron micrographs of spermatozoa (1–4) and spermatid head (5–8); head and sheath morphology (1 and 2) and acrosome (3 and 4) (*white arrows*) from α1AMPK$^{+/+}$ (1 and 3) and α1AMPK$^{-/-}$ mice (2 and 4). Irregular nuclei of spermatids were observed in α1AMPK$^{-/-}$ mice (6 and 8) (*white arrows*) compared with α1AMPK$^{+/+}$ mice (5 and 7). *Scale bar*, 2 μm.

normal spermatozoa with curved sheaths tended to be higher in homozygous α1AMPK KO mice compared with α1AMPK wild-type mice ($P = 0.05$) (Fig. 3E). Transmission electron microscopy analysis confirmed the neck abnormality without acrosome alteration (Fig. 3, F1–F4) and has shown disturbances during head formation (Fig. 3, F5–F8). These results indicate a decrease in the quality but not in the production of spermatozoa in α1AMPK KO mice.

Mitochondrial defect reduces motility of α1AMPK$^{-/-}$ spermatozoa

Sperm analysis performed with an integrated visual optical system (IVOS) analyzer showed a 1.7-fold increase in static spermatozoa and a 2.4-fold reduction in rapid spermatozoa in α1AMPK KO mice compared with wild-type mice (Fig. 4A, $P < 0.05$). In α1AMPK KO mice, spermatozoa also exhibited a decrease in velocity (Fig. 4B) (α1AMPK KO mice, 186 μm/sec; α1AMPK wild-type mice, 252 μm/sec; $P < 0.05$).

Because spermatozoa motility is strongly associated with activity of mitochondria localized in the midpiece (62), sperm mitochondria were evaluated by testing mitochondrial membrane potential, measurement of the mitochondrial respiration, and microscopic ultrastructural analysis. The percentage of active mitochondria with a high polarization tended to be reduced to about half in semen from α1AMPK KO mice ($P = 0.07$, Fig. 4C). In addition, the measurement of the mitochondrial respiration validated our preliminary results because we found a reduction of the oxygen consumption in α1AMPK KO spermatozoa compared with α1AMPK wild-type spermatozoa in all the conditions tested. α1AMPK KO spermatozoa presented significantly lower basal JO_2 rates of 60% (α1AMPK wild-type spermatozoa, 2.19 pmol O_2/sec · 10^6 cells; α1AMPK KO spermatozoa, 0.81 pmol O_2/sec · 10^6 cells cells, $P < 0.05$) (Fig. 4D). In addition, oligomycin-sensitive and maximal JO_2 were also diminished by 50 and 30% but without reaching statistical significance. Furthermore, ultrastructural studies of α1AMPK KO sperm have shown a decrease in the number of mitochondria as illustrated in transverse sections of the midpiece region of spermatozoa (Fig. 4E, $P < 0.001$) and a 3-fold increase in the percentage of mitochondria exhibiting dilated intermembrane space (*black arrows*) in contrast to wild-type sperm (Fig. 4F, $P < 0.05$). During spermiogenesis, abnormal arrangement of mitochondria along microtubules in the midpiece was also observed in α1AMPK KO mice (Fig. 4G). In addition, the total

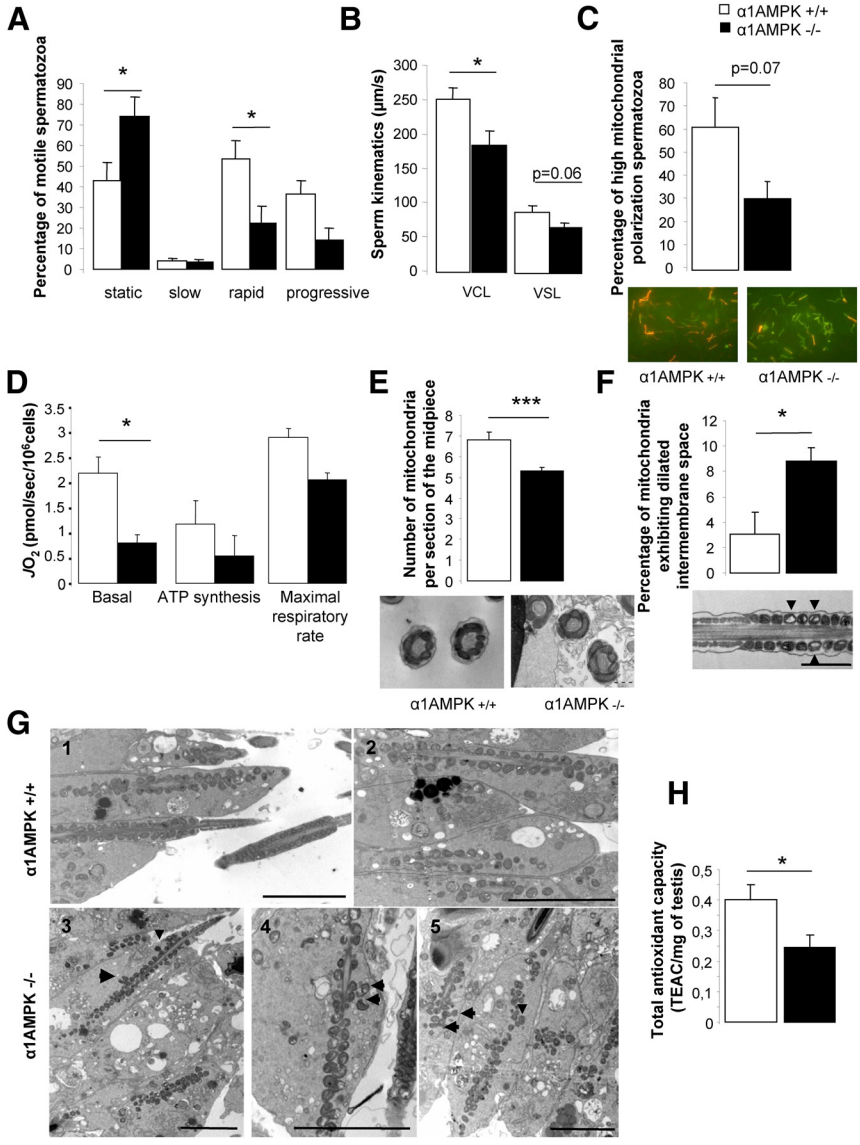

FIG. 4. Analysis of spermatozoa mobility and characterization of mitochondria. Sperm mobility parameters, percentage of motile spermatozoa (A) and sperm kinematics (B) of α1AMPK$^{+/+}$ mice (n = 6) and α1AMPK$^{-/-}$ mice (n = 6), were performed by computer-assisted sperm analysis. VCL, Sperm curvilinear velocity; VSL, sperm straight-line velocity. *, $P < 0.05$. C, Mitochondrial activity was determined by JC-1 staining and represented by percentage of high mitochondrial polarization spermatozoa (orange/red fluorescence) in α1AMPK$^{+/+}$ mice (n = 5) and α1AMPK$^{-/-}$ mice (n = 5). Low mitochondrial membrane potential was observed in green fluorescence. D, Spermatozoa suspension (2×10^6 cells/ml) in M2 medium supplemented with 5 mM sodium pyruvate was transferred immediately, after isolation, into a stirrer 2-ml oxygraph vessel where JO_2 was recorded before and after the successive addition of 0.5 μg/ml oligomycin and 1–2 μM carbonyl cyanide *m*-chlorophenylhydrazone. Data are represented as means ± SEM of n = 3 different spermatozoa isolations in which measurements were performed in duplicate. *, $P < 0.05$. E, The number of mitochondria per section of spermatozoa in the midpiece from α1AMPK$^{+/+}$ mice (n = 5) and α1AMPK$^{-/-}$ mice (n = 5). *Scale bar*, 500 nm. F, Percentage of mitochondria exhibiting partial or total cristolysis was measured on transmission electron micrographs. *Black arrows* indicate crystolysis in mitochondria. *Scale bar*, 1 μm. G, Testis micrographs from α1AMPK$^{-/-}$ mice (3–5) exhibited abnormal arrangement of mitochondria (*arrowhead*) during midpiece formation in the testis compared with α1AMPK wild-type mice (1 and 2). *Scale bar*, 5 μm. H, Intratesticular antioxidant activity measured in units called Trolox equivalent antioxidant capacity (TEAC) per milligram of testis. Data are represented as mean or percentage ± SEM. *, $P < 0.05$; ***, $P < 0.001$.

antioxidant capacity in the whole testis was lower in α1AMPK$^{-/-}$ mice (Fig. 4H, $P < 0.05$).

Hyperandrogenism in male α1AMPK$^{-/-}$ mice

Plasma testosterone levels were about twice as high in α1AMPK KO mice (Fig. 5A, $P < 0.05$) and more than 3-fold higher in testicular extract (Fig. 5C, $P < 0.01$) compared with α1AMPK wild-type mice. Hyperandrogenism was not associated with an alteration of the plasma cortisol level (Fig. 5B) or an increase in the number of Leydig cells in the α1AMPK KO mice (Fig. 5D). However, the mean volume of the Leydig cell was significantly increased (Fig. 5E). At the ultrastructural level, Leydig cells from α1AMPK KO mice exhibited an alteration of the surface occupied by smooth endoplasmic reticulum (SER), involved in synthesis of lipids and steroids, and the presence of larger structures of membranous whorls of SER compared with wild-type mice (Fig. 5F). Additionally, α1AMPK KO mice presented a 5-fold increase in intratesticular cholesterol concentration, a precursor for steroid synthesis (Fig. 6A, $P < 0.01$). The protein level of a cholesterol carrier (StAR) and two enzymes involved in steroid production (P450c17 and 3βHSD) was higher in α1AMPK KO testicular extract (1.9-, 3.1-, and 1.8-fold increase in α1AMPK$^{-/-}$ compared with wild-type mice, respectively) (Fig. 6B). This result was associated with an increase in phosphorylation of the CREB transcription factor in Leydig cells (Fig. 6C, $P < 0.001$). Phosphorylation of serine 133 is known to activate CREB and induce transcription of target genes such as StAR and 3βHSD. Hyperphosphorylation of CREB was also observed on a basal level in purified cultured α1AMPK KO Sertoli cells (1.5-fold increase, Fig. 6D).

To test whether the higher CREB activity is due to stimulation of the gonadotropin receptor pathway (a G

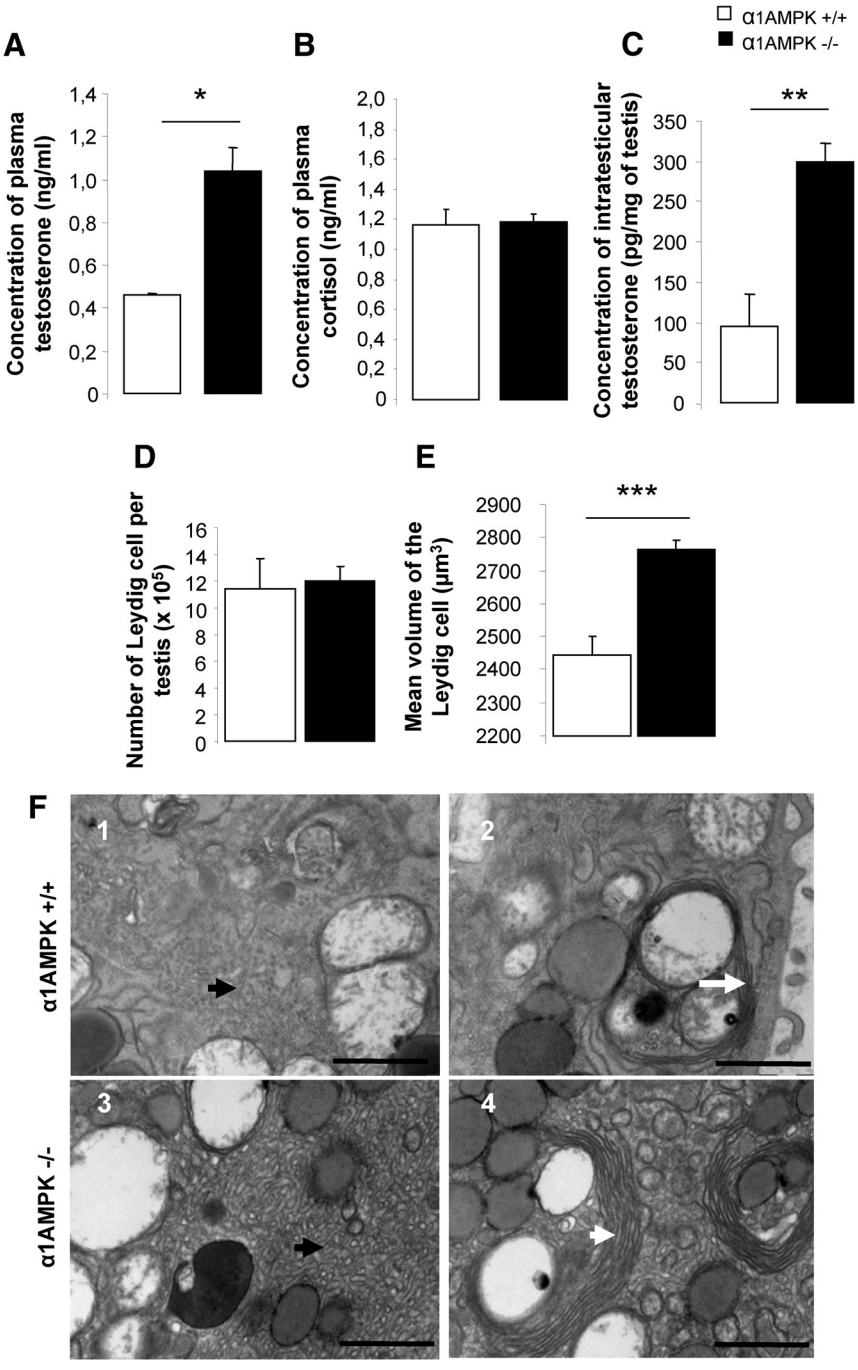

FIG. 5. A–C, Hyperandrogenism in α1AMPK$^{-/-}$ male. Plasma concentrations of testosterone (A), cortisol (B), and intratesticular concentrations of testosterone (C) in α1AMPK$^{+/+}$ mice (n = 5) and α1AMPK$^{-/-}$ mice (n = 5) were analyzed. *, $P < 0.05$; **, $P < 0.01$. D and E, The number of Leydig cells (D) and their mean cell volume (E) were estimated in α1AMPK$^{+/+}$ (n = 3) and α1AMPK$^{-/-}$ testis (n = 5). ***, $P < 0.001$. Data are represented as mean or percentage ± SEM. F, Transmission electron micrographs of Leydig cells; 1 and 3, altered surface occupied by SER (*black arrows*) in α1AMPK$^{-/-}$ Leydig cells; 2 and 4, increase in size of membranous whorls of SER (*white arrows*) in α1AMPK$^{-/-}$ Leydig cells. *Scale bar*, 1 μm.

protein-coupled receptor, cAMP-dependent pathway), the cAMP concentration was measured in the freshly recovered testis (Fig. 6E) and in a culture medium released by purified Sertoli cells (Fig. 6F). In both cases, basal cAMP concentrations were increased in α1AMPK KO mice. The high cAMP testicular concentration is not closely linked to gonadotropin secretion, because LH plasma (α1AMPK KO mice, 0.19 ± 0.02 ng/ml; α1AMPK wild-type mice, 0.26 ± 0.07 ng/ml, $P > 0,05$) and FSH plasma (α1AMPK KO mice, 34.4 ± 2.1 ng/ml; α1AMPK wild-type mice, 38.8 ± 3.1 ng/ml; $P > 0,05$) and pituitary levels (LH: α1AMPK KO mice, 476 ± 142 ng/mg; α1AMPK wild-type mice, 775 ± 237 ng/mg, $P > 0,05$; and FSH: α1AMPK KO mice, 1367 ± 193 ng/mg; α1AMPK wild-type mice, 2790 ± 779 ng/mg, $P = 0,09$) tended to be reduced in α1AMPK KO mice compared with α1AMPK wild-type mice.

Discussion

These data show that inactivation of the AMPKα1 gene reduces male fertility. Indeed, α1AMPK$^{-/-}$ males present a 20% decrease in litter size per pregnancy associated with hyperandrogenism and alteration in morphology and motility of the spermatozoa.

In our study, localization of the α1AMPK expression has been found in germ cells and in Leydig and Sertoli cells in the testis. A previous study has identified AMPK expression in the rat testis (16), and the authors have demonstrated by immunoprecipitation that 75% of the AMPK activity is associated with α1 catalytic subunit and 25% with the α2 AMPK subunit in the whole testis. Furthermore, the kinase of AMPK, LKB1 (27, 47) and two AMPK-related kinases (37), SNRK (35) and MARK2 (36) are also expressed in the testis. Inactivation of these genes induced alterations of fertility and in some case sterility, suggesting that AMPK/AMPK-related activity is involved in testicular function.

The high testosterone level measured in α1AMPK$^{-/-}$ mice could affect spermatogenesis. That disturbance can-

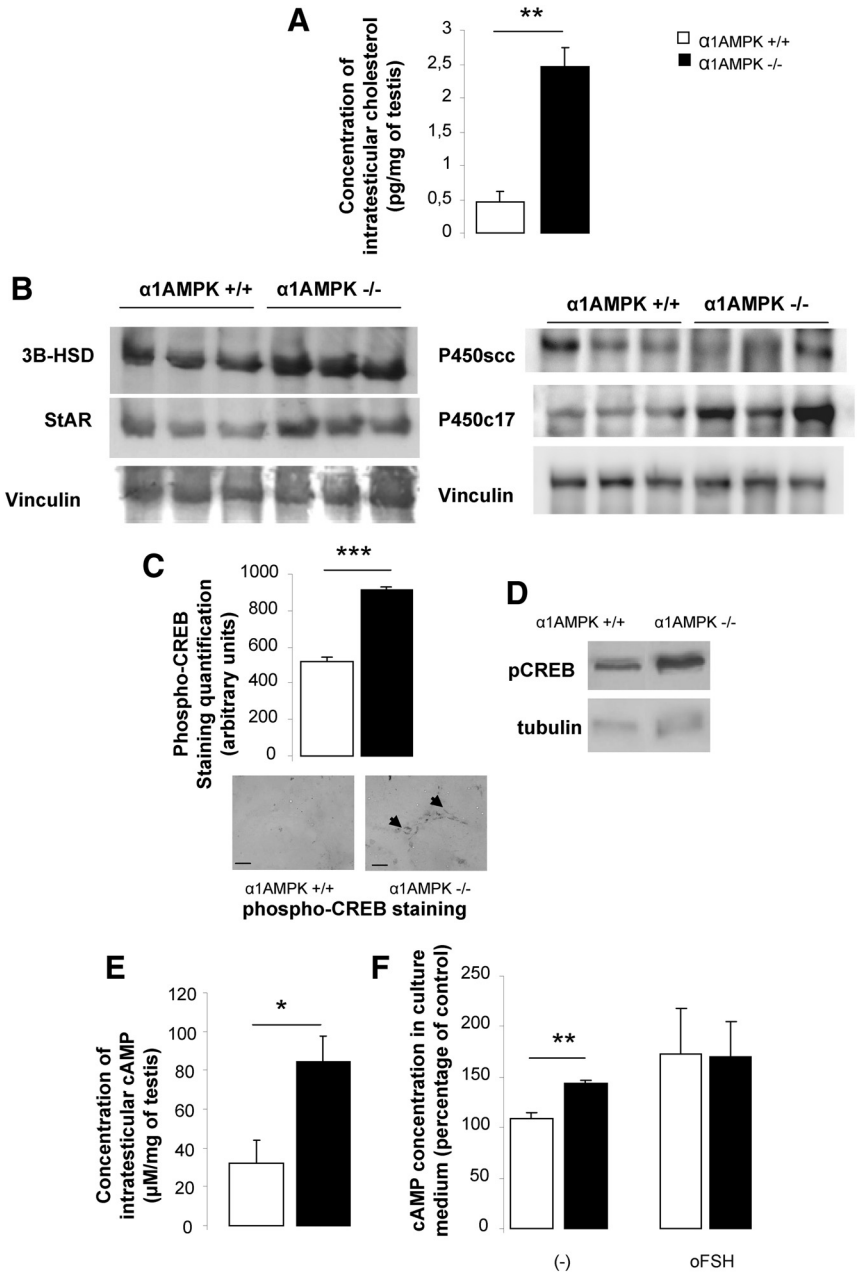

FIG. 6. Molecular alteration in steroidogenesis. A, Intratesticular concentrations of cholesterol in α1AMPK$^{+/+}$ (n = 5) and α1AMPK$^{-/-}$ mice (n = 5). **, $P < 0.01$. B, Western blot analysis of StAR, 3β-HSD, P450c17, and P450scc expression in α1AMPK$^{+/+}$ (lanes 1–3, three different animals) and α1AMPK$^{-/-}$ testis (lanes 4–6, three different animals), normalized to vinculin. C, Quantification of phospho-CREB immunostaining intensity localized in Leydig cells. Bright-field photomicrographs are shown below the *bar graph*. *Scale bar*, 20 μm; n = 3 per genotype. ***, $P < 0.001$. D, Western blot analysis of phospho-CREB expression in purified Sertoli cells culture of α1AMPK$^{+/+}$ and α1AMPK$^{-/-}$ mice. Tubulin served as a loading control. Results are representative of three independent experiments. E, Intratesticular cAMP concentration from α1AMPK$^{+/+}$ mice (n = 5) and α1AMPK$^{-/-}$ mice (n = 6). *, $P < 0.05$. F, cAMP concentration in culture medium of Sertoli cells stimulated for 15 min with or without ovine FSH (oFSH) (100 ng/ml) (percentage of control normalized per 200,000 cells/wells; n = 4 independent experiments). **, $P < 0.01$. Data are represented as mean or percentage ± SEM.

not be attributed to adrenal gland disorders or to glucocorticoid resistance (Fig. 5B) but was associated with hyperactive Leydig cells as attested by the increased mean volume, the altered endoplasmic reticulum area, the high intratesticular cholesterol concentration, and the strong expression of proteins involved in steroid production. These results could be linked to studies that have described the activation of AMPK complexes by natural activators like curcumin (63, 64) or resveratrol (65, 66) that inhibit androgen production by Leydig cells. In the rat ovary, activation of AMPK reduces progesterone secretion in granulosa cells by inhibition of expression of the 3βHSD enzyme (67) but not p450scc as observed in our model. Furthermore, high intratesticular cAMP concentrations associated with high phosphorylation of CREB suggested that gonadotropin receptors and/or a downstream signaling pathway could be activated at a basal level, despite recent work that described expression of AMPK in rat gonadotrope pituitary cells (60). In our model, LH and FSH pituitary concentrations appeared lower than in wild-type mice (1.6- to 2-fold), suggesting that androgen levels induced negative feedback on gonadotropin synthesis rather than absence of AMPK affecting gonadotropin secretion. Indeed, Tosca *et al.* (60) have shown that inhibition of AMPK by a synthetic inhibitor, compound C, did not affect LH and FSH secretions in gonadotrope cell lines.

Additionally, different models with high testosterone levels indicate alteration of sperm quality (68, 69). Conditional deletion of α1AMPK in Leydig cells or administration of antiandrogen treatment should be helpful to clarify the role of testosterone in sperm quality in these transgenic mice.

In various cells, AMPK has been shown to be involved in mitochondrial function. In their work, Nakada *et al.* (70) showed that spermatogenesis is closely linked to mitochondrial respiration, and in a recent publication, Pelliccione *et al.* (71) associated asthenozoospermia with abnormal mitochondrial ultrastructure. Thus, we hypothesize that the motility disturbance observed in our α1AMPK KO model and in the LKB1 KO model (an AMPK kinase) showing a strong spermatozoa abnormal-

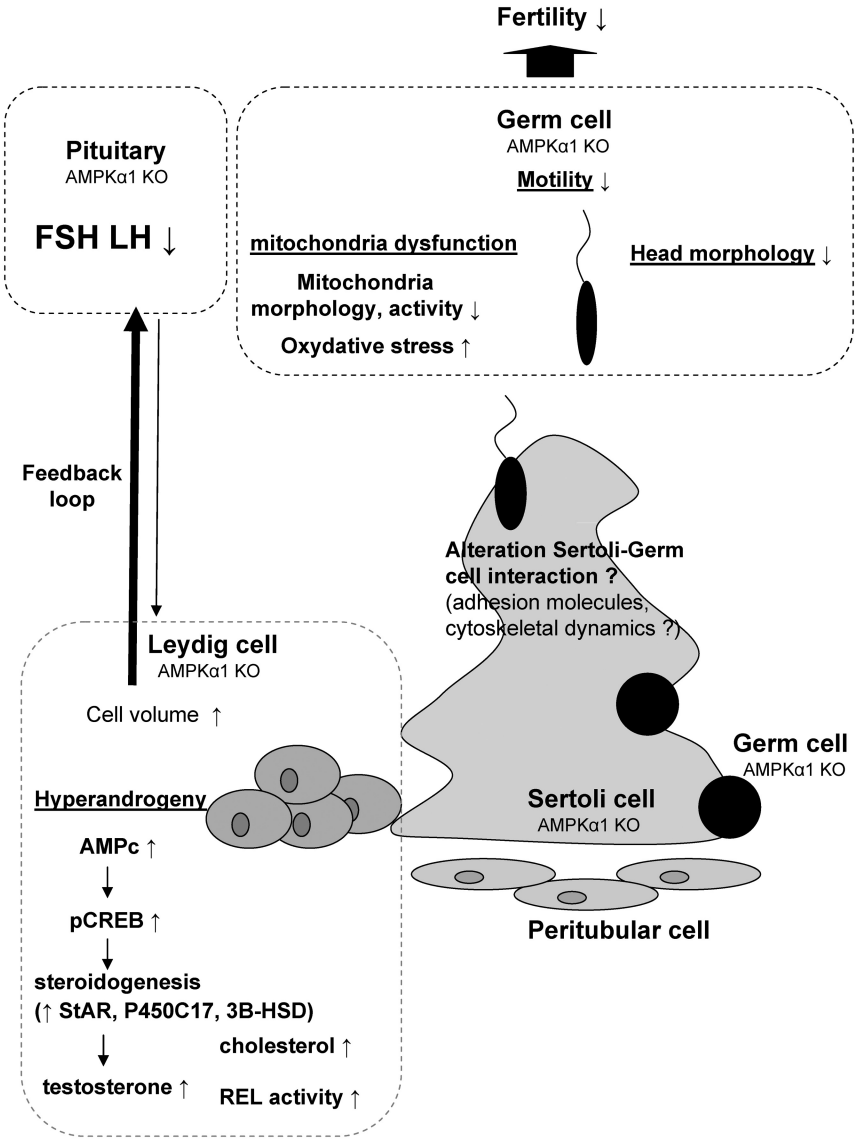

FIG. 7. α1AMPK deletion: schematic summary of the consequences on male fertility.

ity (motility and head morphology) (47) was directly linked to mitochondrial dysgenesis. Our hypothesis seems to be confirmed, because investigation of mitochondrial integrity in α1AMPK KO sperm mice has demonstrated a 50% reduction in mitochondrial activity, a decrease in their number per sheath section, and a 3-fold rise in abnormal mitochondria with dilated intermembrane space structure. Moreover, in his work, Jäger *et al.* (72) noted that AMPK activation is required for peroxisome-proliferator-activated receptor γ coactivator 1α (PGC-1α) activation, a key regulator of mitochondrial biogenesis (73), and a study of Rodríguez-Cuenca *et al.* (74) showed that testosterone reduces PGC-1α mRNA levels. Therefore, in our model, the substantial rise in testosteronemia and absence of α1AMPK in spermatozoa could hardly reduce PGC-1α expression and mitochondrial biogenesis. A dysfunction of mitochondria that could also induce a high oxidative stress has been described in red blood cells from α1AMPK KO mice (75). Similarly, we have measured a lower total antioxidant capacity in the α1AMPK$^{-/-}$ testis. Strangely, a mouse model inactivated for an oxidative-stress sensor proteins like glutathione peroxidase 4 (76, 77) is described with structural abnormalities in spermatozoa closely similar to those observed in α1AMPK KO. Furthermore, these mitochondrial malfunctions were not due to a decline in available energy as lactate substrate, produced by Sertoli cells (78), because as shown in Fig. 2, lactate production *in vivo* and *in vitro* (even after metformin induction) by Sertoli cells was similar in α1AMPK KO and wild-type mice.

The Sertoli cells, closely linked to germ cells, have an essential role in the shaping of the spermatid head (79). Although α1AMPK KO Sertoli cells did not present abnormalities in structure and nucleus polarization (Supplemental Fig. 2), observations of abnormalities in sperm maturation (mitochondria organization and head shape formation at the spermatid stage) suggest a role of AMPK in the cytoskeletal dynamics. Observations from transmission electron microscopy of elongated spermatids have confirmed the presence of some disrupted Sertoli cell/germ cell junctions in α1AMPK-defective testis (Supplemental Fig. 3). In a recent study, Galardo *et al.* (80) demonstrated that AMPK affects some adhesion molecule expression and influences junction complex integrity in rat Sertoli cells. Moreover, mice deleted for adhesion molecules present in Sertoli/germ cell junctions, like nectin-2 (81) or tumor suppressor in lung cancer 1 (82) confirmed the essential role of these molecules for sperm head configuration, midpiece formation, and sperm motility. Thus, we can think that AMPK has a potential role in the cytoskeletal interaction between Sertoli and germ cells, leading to an abnormal head shape and mitochondrial organization around microtubules.

In conclusion, inactivation of the α1AMPK predominant isoform in somatic and germ cells has shown a major malfunction of mitochondrial activity, leading mainly to a decrease in sperm quality (morphology and mobility) and alteration of steroid production as described in Fig. 7.

Hence, the use of an AMPK activator such as metformin, an insulin sensitizer used in the therapeutic management of type 2 diabetes mellitus, raises the question of its potential consequences in human male fertility.

Acknowledgments

We thank Dr. Dale Buchanan Hales (Department of Physiology and Biophysics, University of Illinois at Chicago, Chicago, IL) and Dr. Grahame Hardie (University of Dundee, Dundee, UK) for generously providing the anti-StAR, anti-p450scc, and anti-α1- and -α2AMPK antibodies, respectively and Alan Scaife for the manuscript editing.

Address all correspondence and requests for reprints to: Dr. Pascal Froment Ph.D, Team Testicule Ontogenèse et Métabolisme Energétique, Institut National de la Recherche Agronomique, Station de Recherche Avicole, 37380 Nouzilly, France. E-mail: pfroment@tours.inra.fr.

This work was partly supported by the national program called FERTiNERGY funded by the French National Research Agency and by the European Commission integrated project (LSHM-CT-2004-005272). P.T. was supported by a French fellowship from the Ministère de l'éducation et de la recherche and N.S. by a postdoctoral fellowship (Grant 2010 BLAN 1123) from the French National Research Agency.

Disclosure Summary: The authors have nothing to disclose.

References

1. **ESHRE Capri Workshop Group** 2006 Nutrition and reproduction in women. Hum Reprod Update 12:193–207
2. **Mah PM, Wittert GA** 2010 Obesity and testicular function. Mol Cell Endocrinol 316:180–186
3. **Monget P, Martin GB** 1997 Involvement of insulin-like growth factors in the interactions between nutrition and reproduction in female mammals. Hum Reprod 12(Suppl 1):33–52
4. **Barash IA, Cheung CC, Weigle DS, Ren H, Kabigting EB, Kuijper JL, Clifton DK, Steiner RA** 1996 Leptin is a metabolic signal to the reproductive system. Endocrinology 137:3144–3147
5. **Combs TP, Pajvani UB, Berg AH, Lin Y, Jelicks LA, Laplante M, Nawrocki AR, Rajala MW, Parlow AF, Cheeseboro L, Ding YY, Russell RG, Lindemann D, Hartley A, Baker GR, Obici S, Deshaies Y, Ludgate M, Rossetti L, Scherer PE** 2004 A transgenic mouse with a deletion in the collagenous domain of adiponectin displays elevated circulating adiponectin and improved insulin sensitivity. Endocrinology 145:367–383
6. **Brüning JC, Gautam D, Burks DJ, Gillette J, Schubert M, Orban PC, Klein R, Krone W, Müller-Wieland D, Kahn CR** 2000 Role of brain insulin receptor in control of body weight and reproduction. Science 289:2122–2125
7. **Burks DJ, Font de Mora J, Schubert M, Withers DJ, Myers MG, Towery HH, Altamuro SL, Flint CL, White MF** 2000 IRS-2 pathways integrate female reproduction and energy homeostasis. Nature 407:377–382
8. **Giguère V** 1999 Orphan nuclear receptors: from gene to function. Endocr Rev 20:689–725
9. **Frenoux JM, Vernet P, Volle DH, Britan A, Saez F, Kocer A, Henry-Berger J, Mangelsdorf DJ, Lobaccaro JM, Drevet JR** 2004 Nuclear oxysterol receptors, LXRs, are involved in the maintenance of mouse caput epididymidis structure and functions. J Mol Endocrinol 33:361–375
10. **Robertson KM, Schuster GU, Steffensen KR, Hovatta O, Meaney S, Hultenby K, Johansson LC, Svechnikov K, Söder O, Gustafsson JA** 2005 The liver X receptor-β is essential for maintaining cholesterol homeostasis in the testis. Endocrinology 146:2519–2530
11. **Bełtowski J, Semczuk A** 2010 Liver X receptor (LXR) and the reproductive system: a potential novel target for therapeutic intervention. Pharmacol Rep 62:15–27
12. **Repa JJ, Turley SD, Lobaccaro JA, Medina J, Li L, Lustig K, Shan B, Heyman RA, Dietschy JM, Mangelsdorf DJ** 2000 Regulation of absorption and ABC1-mediated efflux of cholesterol by RXR heterodimers. Science 289:1524–1529
13. **Kastner P, Mark M, Leid M, Gansmuller A, Chin W, Grondona JM, Décimo D, Krezel W, Dierich A, Chambon P** 1996 Abnormal spermatogenesis in RXRβ mutant mice. Genes Dev 10:80–92
14. **Fredrikson G, Strålfors P, Nilsson NO, Belfrage P** 1981 Hormone-sensitive lipase of rat adipose tissue. Purification and some properties. J Biol Chem 256:6311–6320
15. **Chung S, Wang SP, Pan L, Mitchell G, Trasler J, Hermo L** 2001 Infertility and testicular defects in hormone-sensitive lipase-deficient mice. Endocrinology 142:4272–4281
16. **Cheung PC, Salt IP, Davies SP, Hardie DG, Carling D** 2000 Characterization of AMP-activated protein kinase gamma-subunit isoforms and their role in AMP binding. Biochem J 346(Pt 3):659–669
17. **Kahn BB, Alquier T, Carling D, Hardie DG** 2005 AMP-activated protein kinase: ancient energy gauge provides clues to modern understanding of metabolism. Cell Metab 1:15–25
18. **Hardie DG, Hawley SA, Scott JW** 2006 AMP-activated protein kinase–development of the energy sensor concept. J Physiol 574:7–15
19. **Kola B, Boscaro M, Rutter GA, Grossman AB, Korbonits M** 2006 Expanding role of AMPK in endocrinology. Trends Endocrinol Metab 17:205–215
20. **Cantó C, Auwerx J** 2010 AMP-activated protein kinase and its downstream transcriptional pathways. Cell Mol Life Sci 67:3407–3423
21. **Bouly JP, Gissot L, Lessard P, Kreis M, Thomas M** 1999 Arabidopsis thaliana proteins related to the yeast SIP and SNF4 interact with AKINα1, an SNF1-like protein kinase. Plant J 18:541–550
22. **Woods A, Munday MR, Scott J, Yang X, Carlson M, Carling D** 1994 Yeast SNF1 is functionally related to mammalian AMP-activated protein kinase and regulates acetyl-CoA carboxylase in vivo. J Biol Chem 269:19509–19515
23. **Steinke D, Salzburger W, Braasch I, Meyer A** 2006 A Many genes in fish have species-specific asymmetric rates of molecular evolution. BMC Genomics 7:20
24. **Proszkowiec-Weglarz M, Richards MP, Ramachandran R, McMurtry JP** 2006 Characterization of the AMP-activated protein kinase pathway in chickens. Comp Biochem Physiol B Biochem Mol Biol 143:92–106
25. **Stapleton D, Mitchelhill KI, Gao G, Widmer J, Michell BJ, Teh T, House CM, Fernandez CS, Cox T, Witters LA, Kemp BE** 1996 Mammalian AMP-activated protein kinase subfamily. J Biol Chem 271:611–614
26. **Suter M, Riek U, Tuerk R, Schlattner U, Wallimann T, Neumann D** 2006 Dissecting the role of 5′-AMP for allosteric stimulation, activation, and deactivation of AMP-activated protein kinase. J Biol Chem 281:32207–32216
27. **Woods A, Johnstone SR, Dickerson K, Leiper FC, Fryer LG, Neumann D, Schlattner U, Wallimann T, Carlson M, Carling D** 2003 LKB1 is the upstream kinase in the AMP-activated protein kinase cascade. Curr Biol 13:2004–2008
28. **Hawley SA, Pan DA, Mustard KJ, Ross L, Bain J, Edelman AM, Frenguelli BG, Hardie DG** 2005 Calmodulin-dependent protein ki-

nase kinase-β is an alternative upstream kinase for AMP-activated protein kinase. Cell Metab 2:9–19

29. **Xie M, Zhang D, Dyck JR, Li Y, Zhang H, Morishima M, Mann DL, Taffet GE, Baldini A, Khoury DS, Schneider MD** 2006 A pivotal role for endogenous TGF-β-activated kinase-1 in the LKB1/AMP-activated protein kinase energy-sensor pathway. Proc Natl Acad Sci USA 103:17378–17383
30. **Costanzo-Garvey DL, Pfluger PT, Dougherty MK, Stock JL, Boehm M, Chaika O, Fernandez MR, Fisher K, Kortum RL, Hong EG, Jun JY, Ko HJ, Schreiner A, Volle DJ, Treece T, Swift AL, Winer M, Chen D, Wu M, Leon LR, Shaw AS, McNeish J, Kim JK, Morrison DK, Tschöp MH, Lewis RE** 2009 KSR2 is an essential regulator of AMP kinase, energy expenditure, and insulin sensitivity. Cell Metab 10:366–378
31. **Minokoshi Y, Kim YB, Peroni OD, Fryer LG, Müller C, Carling D, Kahn BB** 2002 Leptin stimulates fatty-acid oxidation by activating AMP-activated protein kinase. Nature 415:339–343
32. **Yamauchi T, Kamon J, Minokoshi Y, Ito Y, Waki H, Uchida S, Yamashita S, Noda M, Kita S, Ueki K, Eto K, Akanuma Y, Froguel P, Foufelle F, Ferre P, Carling D, Kimura S, Nagai R, Kahn BB, Kadowaki T** 2002 Adiponectin stimulates glucose utilization and fatty-acid oxidation by activating AMP-activated protein kinase. Nat Med 8:1288–1295
33. **Manning G, Whyte DB, Martinez R, Hunter T, Sudarsanam S** 2002 The protein kinase complement of the human genome. Science 298: 1912–1934
34. **Lizcano JM, Göransson O, Toth R, Deak M, Morrice NA, Boudeau J, Hawley SA, Udd L, Mäkelä TP, Hardie DG, Alessi DR** 2004 LKB1 is a master kinase that activates 13 kinases of the AMPK subfamily, including MARK/PAR-1. EMBO J 23:833–843
35. **Jaleel M, McBride A, Lizcano JM, Deak M, Toth R, Morrice NA, Alessi DR** 2005 Identification of the sucrose non-fermenting related kinase SNRK, as a novel LKB1 substrate. FEBS Lett 579:1417–1423
36. **Bessone S, Vidal F, Le Bouc Y, Epelbaum J, Bluet-Pajot MT, Darmon M** 1999 EMK protein kinase-null mice: dwarfism and hypofertility associated with alterations in the somatotrope and prolactin pathways. Dev Biol 214:87–101
37. **Bright NJ, Thornton C, Carling D** 2009 The regulation and function of mammalian AMPK-related kinases. Acta Physiol (Oxf) 196: 15–26
38. **Tosca L, Chabrolle C, Uzbekova S, Dupont J** 2007 Effects of metformin on bovine granulosa cells steroidogenesis: possible involvement of adenosine 5′ monophosphate-activated protein kinase (AMPK). Biol Reprod 76:368–378
39. **Karlsson C, Lindell K, Svensson E, Bergh C, Lind P, Billig H, Carlsson LM, Carlsson B** 1997 Expression of functional leptin receptors in the human ovary. J Clin Endocrinol Metab 82:4144–4148
40. **Chabrolle C, Tosca L, Dupont J** 2007 Regulation of adiponectin and its receptors in rat ovary by human chorionic gonadotrophin treatment and potential involvement of adiponectin in granulosa cell steroidogenesis. Reproduction 133:719–731
41. **Tena-Sempere M, Barreiro ML** 2002 Leptin in male reproduction: the testis paradigm. Mol Cell Endocrinol 188:9–13
42. **Caminos JE, Nogueiras R, Gaytán F, Pineda R, González CR, Barreiro ML, Castaño JP, Malagón MM, Pinilla L, Toppari J, Diéguez C, Tena-Sempere M** 2008 Novel expression and direct effects of adiponectin in the rat testis. Endocrinology 149:3390–3402
43. **Pierre P, Froment P, Nègre D, Ramé C, Barateau V, Chabrolle C, Lecomte P, Dupont J** 2009 Role of adiponectin receptors, AdipoR1 and AdipoR2, in the steroidogenesis of the human granulosa tumor cell line, KGN. Hum Reprod 24:2890–2901
44. **Chabrolle C, Tosca L, Ramé C, Lecomte P, Royère D, Dupont J** 2009 Adiponectin increases insulin-like growth factor I-induced progesterone and estradiol secretion in human granulosa cells. Fertil Steril 92:1988–1996
45. **Chen J, Hudson E, Chi MM, Chang AS, Moley KH, Hardie DG, Downs SM** 2006 AMPK regulation of mouse oocyte meiotic resumption in vitro. Dev Biol 291:227–238
46. **Galardo MN, Riera MF, Pellizzari EH, Cigorraga SB, Meroni SB** 2007 The AMP-activated protein kinase activator, 5-aminoimidazole-4-carboxamide-1-b-D-ribonucleoside, regulates lactate production in rat Sertoli cells. J Mol Endocrinol 39:279–288
47. **Towler MC, Fogarty S, Hawley SA, Pan DA, Martin DM, Morrice NA, McCarthy A, Galardo MN, Meroni SB, Cigorraga SB, Ashworth A, Sakamoto K, Hardie DG** 2008 A novel short splice variant of the tumour suppressor LKB1 is required for spermiogenesis. Biochem J 416:1–14
48. **Jørgensen SB, Viollet B, Andreelli F, Frøsig C, Birk JB, Schjerling P, Vaulont S, Richter EA, Wojtaszewski JF** 2004 Knockout of the $\alpha 2$ but not $\alpha 1$ 5′-AMP-activated protein kinase isoform abolishes 5-aminoimidazole-4-carboxamide-1-β-4-ribofuranosidebut not contraction-induced glucose uptake in skeletal muscle. J Biol Chem 279:1070–1079
49. **Rivkees SA, Hall DA, Boepple PA, Crawford JD** 1987 Accuracy and reproducibility of clinical measures of testicular volume. J Pediatr 110:914–917
50. **Froment P, Staub C, Hembert S, Pisselet C, Magistrini M, Delaleu B, Seurin D, Levine JE, Johnson L, Binoux M, Monget P** 2004 Reproductive abnormalities in human insulin-like growth factor-binding protein-1 transgenic male mice. Endocrinology 145:2080–2091
51. **Yamamoto CM, Hikim AP, Lue Y, Portugal AM, Guo TB, Hsu SY, Salameh WA, Wang C, Hsueh AJ, Swerdloff RS** 2001 Impairment of spermatogenesis in transgenic mice with selective overexpression of Bcl-2 in the somatic cells of the testis. J Androl 22:981–991
52. **Toure A, Morin L, Pineau C, Becq F, Dorseuil O, Gacon G** 2001 Tat1, a novel sulfate transporter specifically expressed in human male germ cells and potentially linked to RhoGTPase signaling. J Biol Chem 276:20309–20315
53. **Froment P, Vigier M, Nègre D, Fontaine I, Beghelli J, Cosset FL, Holzenberger M, Durand P** 2007 Inactivation of the IGF-I receptor gene in primary Sertoli cells highlights the autocrine effects of IGF-I. J Endocrinol 194:557–568
54. **Papaioannou V, Johnson R** 1993 Production of chimeras and genetically defined offspring from targeted ES cells. In: Joyner AL, ed. Gene targeting: a practical approach. Oxford, UK: IRL Press; 107–146
55. **Jégou B, Velez de la Calle JF, Bauché F** 1991 Protective effect of medroxyprogesterone acetate plus testosterone against radiation-induced damage to the reproductive function of male rats and their offspring. Proc Natl Acad Sci USA 88:8710–8714
56. **Mukai C, Okuno M** 2004 Glycolysis plays a major role for adenosine triphosphate supplementation in mouse sperm flagellar movement. Biol Reprod 71:540–547
57. **Hochereau-de Reviers MT, Perreau C, Pisselet C, Fontaine I, Monet-Kuntz C** 1990 Comparisons of endocrinological and testis parameters in 18-month-old Ile de France and Romanov rams. Domest Anim Endocrinol 7:63–73
58. **Orgeur P, Naciri N, Yvore P, Bernard S, Nowak R, Schaal B, Lévy F** 1998 Artificial weaning in sheep: consequences on behavioural, hormonal and immuno-pathological indicators of welfare. Appl Anim Behav Sci 58:87–103
59. **McNeilly JR, Brown P, Mullins J, Clark AJ, McNeilly AS** 1996 Characterization of the ovine LH β-subunit gene: the promoter is regulated by GnRH and gonadal steroids in transgenic mice. J Endocrinol 151:481–489
60. **Tosca L, Froment P, Rame C, McNeilly JR, McNeilly AS, Maillard V, Dupont J** 2011 Metformin decreases GnRH- and activin-induced gonadotropin secretion in rat pituitary cells: potential involvement of adenosine 5′ monophosphate-activated protein kinase (PRKA). Biol Reprod 84:351–362
61. **Viollet B, Guigas B, Leclerc J, Hebrard S, Lantier L, Mounier R, Andreelli F, Foretz M** 2009 AMP-activated protein kinase in the

regulation of hepatic energy metabolism: from physiology to therapeutic perspectives. Acta Physiol (Oxf) 196:81–98
62. **Marchetti C, Jouy N, Leroy-Martin B, Defossez A, Formstecher P, Marchetti P** 2004 Comparison of four fluorochromes for the detection of the inner mitochondrial membrane potential in human spermatozoa and their correlation with sperm motility. Hum Reprod 19:2267–2276
63. **Kim T, Davis J, Zhang AJ, He X, Mathews ST** 2009 Curcumin activates AMPK and suppresses gluconeogenic gene expression in hepatoma cells. Biochem Biophys Res Commun 388:377–382
64. **Hu GX, Liang G, Chu Y, Li X, Lian QQ, Lin H, He Y, Huang Y, Hardy DO, Ge RS** 2010 Curcumin derivatives inhibit testicular 17β-hydroxysteroid dehydrogenase 3. Bioorg Med Chem Lett 20:2549–2551
65. **Um JH, Park SJ, Kang H, Yang S, Foretz M, McBurney MW, Kim MK, Viollet B, Chung JH** 2010 AMP-activated protein kinase-deficient mice are resistant to the metabolic effects of resveratrol. Diabetes 59:554–563
66. **Svechnikov K, Spatafora C, Svechnikova I, Tringali C, Söder O** 2009 Effects of resveratrol analogs on steroidogenesis and mitochondrial function in rat Leydig cells in vitro. J Appl Toxicol 29:673–680
67. **Tosca L, Froment P, Solnais P, Ferré P, Foufelle F, Dupont J** 2005 Adenosine 5′-monophosphate-activated protein kinase regulates progesterone secretion in rat granulosa cells. Endocrinology 146:4500–4513
68. **Rulli SB, Ahtiainen P, Mäkelä S, Toppari J, Poutanen M, Huhtaniemi I** 2003 Elevated steroidogenesis, defective reproductive organs, and infertility in transgenic male mice overexpressing human chorionic gonadotropin. Endocrinology 144:4980–4990
69. **Recabarren SE, Rojas-García PP, Recabarren MP, Alfaro VH, Smith R, Padmanabhan V, Sir-Petermann T** 2008 Prenatal testosterone excess reduces sperm count and motility. Endocrinology 149:6444–6448
70. **Nakada K, Sato A, Yoshida K, Morita T, Tanaka H, Inoue S, Yonekawa H, Hayashi J** 2006 Mitochondria-related male infertility. Proc Natl Acad Sci USA 103:15148–15153
71. **Pelliccione F, Micillo A, Cordeschi G, D'Angeli A, Necozione S, Gandini L, Lenzi A, Francavilla F, Francavilla S** 2011 Altered ultrastructure of mitochondrial membranes is strongly associated with unexplained asthenozoospermia. Fertil Steril 95:641–646
72. **Jäger S, Handschin C, St-Pierre J, Spiegelman BM** 2007 AMP-activated protein kinase (AMPK) action in skeletal muscle via direct phosphorylation of PGC-1α. Proc Natl Acad Sci USA 104:12017–12022
73. **Wu Z, Puigserver P, Andersson U, Zhang C, Adelmant G, Mootha V, Troy A, Cinti S, Lowell B, Scarpulla RC, Spiegelman BM** 1999 Mechanisms controlling mitochondrial biogenesis and respiration through the thermogenic coactivator PGC-1. Cell 98:115–124
74. **Rodríguez-Cuenca S, Monjo M, Gianotti M, Proenza AM, Roca P** 2007 Expression of mitochondrial biogenesis-signaling factors in brown adipocytes is influenced specifically by 17β-estradiol, testosterone, and progesterone. Am J Physiol Endocrinol Metab 292:E340–E346
75. **Wang S, Dale GL, Song P, Viollet B, Zou MH** 2010 AMPKα1 deletion shortens erythrocyte life span in mice: role of oxidative stress. J Biol Chem 285:19976–19985
76. **Schneider M, Förster H, Boersma A, Seiler A, Wehnes H, Sinowatz F, Neumüller C, Deutsch MJ, Walch A, Hrabé de Angelis M, Wurst W, Ursini F, Roveri A, Maleszewski M, Maiorino M, Conrad M** 2009 Mitochondrial glutathione peroxidase 4 disruption causes male infertility. FASEB J 23:3233–3242
77. **Liang H, Yoo SE, Na R, Walter CA, Richardson A, Ran Q** 2009 Short form glutathione peroxidase 4 is the essential isoform required for survival and somatic mitochondrial functions. J Biol Chem 284:30836–30844
78. **Odet F, Duan C, Willis WD, Goulding EH, Kung A, Eddy EM, Goldberg E** 2008 Expression of the gene for mouse lactate dehydrogenase C (Ldhc) is required for male fertility. Biol Reprod 79:26–34
79. **Kierszenbaum AL, Tres LL** 2004 The acrosome-acroplaxome-manchette complex and the shaping of the spermatid head. Arch Histol Cytol 67:271–284
80. **Galardo MN, Riera MF, Pellizzari EH, Sobarzo C, Scarcelli R, Denduchis B, Lustig L, Cigorraga SB, Meroni SB** 2010 Adenosine regulates Sertoli cell function by activating AMPK. Mol Cell Endocrinol 330:49–58
81. **Mueller S, Rosenquist TA, Takai Y, Bronson RA, Wimmer E** 2003 Loss of nectin-2 at Sertoli-spermatid junctions leads to male infertility and correlates with severe spermatozoan head and midpiece malformation, impaired binding to the zona pellucida, and oocyte penetration. Biol Reprod 69:1330–1340
82. **Surace EI, Strickland A, Hess RA, Gutmann DH, Naughton CK** 2006 Tslc1 (nectin-like molecule-2) is essential for spermatozoa motility and male fertility. J Androl 27:816–825